Hybrid Modeling, Control and Estimation in ABS Applications based on In-Wheel Electric Motors

Ricardo de Castro, João de Sousa, Rui Araújo, F. Lobo Pereira and Diamantino Freitas

Faculty of Engineering, University of Porto

R. Dr. Roberto Frias, 4200-465 Porto, Portugal

{de.castro, jtasso, raraujo, flp, dfreitas}@fe.up.pt

Abstract— **The problems of tire slip control and peak friction estimation for Anti-lock Braking Systems are formulated and solved in the framework of hybrid control techniques. The hybrid systems model of the vehicle dynamics arises from approximating the nonlinear behavior of the tire-road friction coefficient with a Piecewise Linear Function (PLF). The problem of tyre slip control is formulated as an invariance problem. The invariance control problem is solved with the help of a simple hysteretic controller which takes advantage of the fast torque response from the in-wheel electric motor. The controller's properties, such as necessary conditions to ensure invariance, robustness to disturbances, convergence and limit cycle period are analyzed in detail. The problem of the estimating the peak friction for the tire-road interface is solved using properties of the limit cycles arising in the hybrid model. Monitoring the duty cycle, imposed by hysteretic controller, was found to be sufficient to extract information regarding the conditions of adhesion in the road. The controller and estimator were evaluated under variable grip levels, in a vehicle dynamics simulation software, obtaining a good performance for both the tire slip regulation and for the peak friction estimationd.**

I. INTRODUCTION

The contributions of Anti-lock Braking Systems (ABS) to automotive safety are widely acknowledged by car drivers and automobile industry. ABS are instrumental in reducing the braking distance and preventing the loss of "steerability" (ability to turn the vehicle) under heavy braking. However, the design of an ABS is subject to a number of practical issues and unknowns, making this a challenging task. Firstly, the adhesion conditions vary over time, and the ABS should be able to function properly under different types of grip levels (dry, wet, snow, etc.). Secondly, the vehicle longitudinal speed, a key variable in the model, is difficult to measure experimentally, which requires the implementation of observers to estimate this variable [1]. There is also the problem of regulating the wheel slip, which can be performed in three ways: *i)* direct control, if there is reliable information regarding the speed of the vehicle; *ii)* indirect control with the wheel deceleration, when no longitudinal speed estimation is available; *iii)* mixing slip and wheel deceleration control [2]. Traditional braking actuators, based on hydraulic systems, also poses an additional problem, since they have a considerable pure delay.

Conditioned by these difficulties, the first generation of ABS, adopted by the car industry, used threshold based algorithms [1] to indirectly control the slip through the wheel angular deceleration. Such methods, although robust to variations in adherence conditions, are based on heuristic arguments and require an intensive experimental work for tuning [3]. In recent years, several alternatives to the traditional hydraulic braking systems have emerged, with a more solid theoretical background and featuring continuous torque regulation, such as gain schedule LQ control [4], Proportional and Integral (PI) control based on a linearized model [5], sliding mode [6], among-others (see [7] and references therein).

Approaches based on hybrid systems, i.e. models with continuous and discrete states, were also applied successfully to the wheel slip regulation problem. The first hybrid approach consisted in approximating the nonlinear friction curve with a Piecewise Linear Function (PLF), simplifying the mathematical treatment and analysis, and generating simple hybrid models that can be used to synthesize sliding mode controllers [8] or Model Predictive Controllers (MPC) [9]. A second line of hybrid approaches, presented in [3] and [10], maintains the nonlinear vehicle model, but the slip regulation is performed by an automaton (discrete state machine) that manipulates discrete signals to increase/hold/decrease the brake torque. This control strategy usually leads to the introduction of limit cycles in tire slip, which can be shown to have asymptotic stability, and are particularly useful in hydraulic braking systems with ON/OFF dynamics [10].

The present article focuses on the simultaneous application of the two before mentioned hybrid approaches, i.e. model the nonlinear friction curve through a PLF and regulate the slip with an automaton. The slip control was formulated as a state space invariance problem. A hysteretic controller, which can also be seen as a hybrid system, was found to be a good candidate to solve this problem. Unlike the nonlinear approaches presented in [3] [10], the PLF approximation facilitates the analytical study of some controller properties, like the limit cycle and robustness w.r.t disturbances. In addition we introduce a new peak friction estimation scheme. The estimation is based on the properties of the limit cycles resulting from the control actions.

II. VEHICLE MODEL

The dynamic behavior of the vehicle during braking maneuvers was modeled by the simplified quarter car model, widely used in the literature of the area [2]–[5], [8]–[10]. This model assumes some simplifications; for instance only
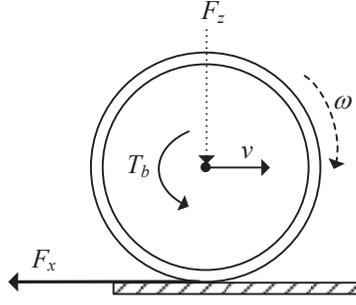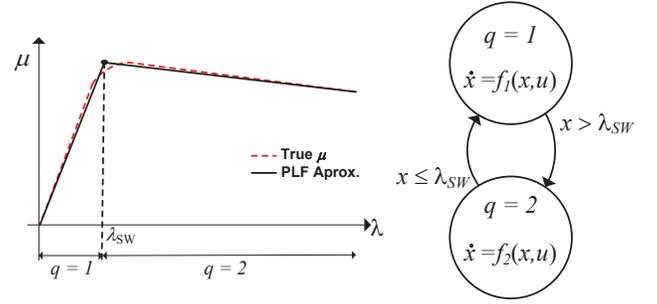
Fig. 1.   Quarter car model.

Fig. 2.   Approximation of the friction coefficient by a Piecewise Linear Function (left) and hybrid model for the quarter car model (right).

longitudinal movement with positive speed ($v>0$) is considered (lateral and vertical motion are neglected), the aerodynamic and rolling resistance forces are ignored, the braking is assume to occur in a straight line (which allow us to assume zero side-slip, simplifying the friction model between tire-road interface), and so on. Although these simplifications reduce the model's accuracy, the main phenomena is conserved and with a more manageable mathematical model. The quarter car dynamics (see Fig. 1) are defined as:

$$J\dot{\omega} = rF_x - T_b \tag{1a}$$
$$M\dot{v} = -F_x \tag{1b}$$

where ω represents the wheel angular speed, v is the longitudinal vehicle speed, T_b is the braking torque applied to the wheel, F_x is the friction force between tire and the road, J is the wheel and transmission inertia , M is the equivalent mass coupled to the wheel and r is the wheel radius.

Modeling the friction force F_x is the main difficulty in the model (1). Generally, the friction force is proportional to the normal force that the wheel supports (F_z) and depends on a nonlinear function $\mu(.)$, known as the friction coefficient, which varies with the longitudinal tire slip (λ) and road adhesion conditions (θ):

$$F_x = F_z\mu(\lambda,\theta) \tag{2}$$
$$\lambda = \frac{v-\omega r}{v} \tag{3}$$

The most popular approaches to represent the friction coefficient $\mu(.)$ are based on two types of models: empirical, such as the "Magic Tyre Formula" [11] or the Burckhardt model [1], and analytical, like the LuGre model [12]. In this work, while the PLF approximation is not applied, the simplified Burckhardt model was used to represent the friction at the tire-road interface:

$$\mu(\lambda,\theta) = \theta_1(1 - e^{-\theta_2\lambda}) - \theta_3\lambda \tag{4}$$

where $\theta = (\theta_1, \theta_2, \theta_3)$ contains the model parameters, which incorporates information on the road adhesion conditions and usually varies in time. For ease of notation, in the rest of the article the parameter θ will be omitted, i.e. $\mu(\lambda,\theta)$ will be replaced by $\mu(\lambda)$, and considered as a perturbation that affects the vehicle dynamics.

The quarter car model, formulated with the vehicle speed v and wheel speed ω as the state variables, is not the more

favorable representation in the context of ABS control. As we attempt to directly control the tire slip λ, it makes sense to reformulate the model in order to include λ as a state variable. By using the algebraic relation between v, ω and λ, the following relation can be established:

$$\dot{\lambda} = \frac{\partial}{\partial t}\left(\frac{v-\omega r}{v}\right) = -\frac{r}{v}\dot{\omega} + \frac{r\omega}{v^2}\dot{v} \tag{5}$$
$$\omega = \frac{v}{r}(1-\lambda) \tag{6}$$

Typically, dynamic models used in traction control systems consider the longitudinal dynamics, expressed by the state variable v, to be much slower than the rotational dynamics of the wheel ω or slip λ. This assumption allows us to replace the state equation (1b) by a parameter v that varies slowly in time [4]. By combining the equations (1a), (2),(5) and (6) we arrive to a modified version of the quarter car model with λ as the unique state variable (and v as a parameter):

$$\dot{\lambda} = -\frac{1}{v}\frac{r}{J}(\Psi(\lambda) - T_b) \tag{7}$$

and the function $\Psi(\lambda)$ is defined by:

$$\Psi(\lambda) = \left(\frac{J}{rM}(1-\lambda) + r\right)F_z\mu(\lambda) \tag{8a}$$
$$\approx rF_z\mu(\lambda) \tag{8b}$$

where the term $J(1-\lambda)/(rM)$ was neglected, given that the mass M is normally much higher than the other parameters [8]. The function $\Psi(\lambda)$ can be interpreted as an equivalent torque applied to the wheel, resulting from the friction force generated at the tire-road interface. Making a simple comparison between $\Psi(\lambda)$ and T_b the vector field direction can be evaluate, i.e. we can determine if λ is increasing or decreasing, and the equilibrium points of the system can also be extracted, equaling $T_b = \Psi(\lambda)$. A discussion about stability of the quarter car model is postponed to Section III, where a hybrid formulation is used to analyze the system properties.

III. HYBRID MODEL

One way to simplify the friction model, suggested in the literature[8][9], is to approximate the nonlinear curve μ by

a Piecewise Linear Function (PLF) divided into N sections:

$$\mu(\lambda) = \mu_q(\lambda) = \begin{cases} \mu_1(\lambda) & \text{if } q = 1 \\ \dots \\ \mu_N(\lambda) & \text{if } q = N \end{cases} \tag{9}$$

The linear functions μ_q, $q \in \mathcal{Q} = \{1,...,N\}$, are obtained linearizing the μ curve around a operation point λ_q^*, based on the first terms of the Taylor series:

$$\mu_q(\lambda) \simeq \mu(\lambda_q^*) + (\lambda - \lambda_q^*) \frac{\partial \mu}{\partial \lambda}\bigg|_{\lambda = \lambda_q^*} \tag{10}$$

$$= \left(\frac{\partial \mu}{\partial \lambda}\bigg|_{\lambda = \lambda_q^*}\right) \lambda + \left(\mu(\lambda_q^*) - \lambda_q^* \frac{\partial \mu}{\partial \lambda}\bigg|_{\lambda = \lambda_q^*}\right) \tag{11}$$

$$= m_q \lambda + c_q \tag{12}$$

where the m_q and c_q represent the slop and offset for each of the PLF sections. Figure 2 presents an example of the approximation of a typical friction curve through a PLF divided in 2 sections ($N = 2$). The first section, $q = 1$, is characterized by a linear increase of μ with λ, and typically has positive slope and zero offset ($m_1 > 0$, $c_1 = 0$). When the slip exceeds a given threshold, λ_{SW}, the second section becomes active, $q = 2$, which is usually characterized by a descending slope and positive offset ($m_2 < 0$, $c_2 > 0$). The switching between sections is defined by the parameter λ_{SW}, corresponding to the slip where the peak friction occurs, and can be defined as:

$$q = \sigma(\lambda) = \begin{cases} 1 & \text{if } \lambda \le \lambda_{SW} \\ 2 & \text{if } \lambda > \lambda_{SW} \end{cases} \tag{13}$$

The representation of the friction coefficient μ by a PLF, implies that the quarter car model (7) contains both a continuous state (slip λ), and a discrete state (representing the section in which the PLF is operating). These kinds of systems, with discrete and continuous states, are known as hybrid systems, which motivates the introduction of the following definition:

Definition 1: A Hybrid System is a collection $H = (\mathcal{Q}, \mathcal{X}, f, \sigma, \rho, \mathcal{U})$, with continuous dynamics $\dot{x} = f(q,x,u)$, discrete evolution $q = \sigma(q^-, x^-)$ and resets: $x = \rho(q^-, x^-)$, where $q \in \mathcal{Q} = \{q_1, q_2, ... q_N\}$ is the discrete state; $x \in \mathcal{X} \subseteq \mathbb{R}^n$ is the continuous state space; $f : \mathcal{Q} \times \mathcal{X} \to \mathbb{R}^n$ is the vector field assigned to each discrete state; $\sigma : \mathcal{Q} \times \mathcal{X} \to \mathcal{Q}$ is the discrete transition, $\rho : \mathcal{Q} \times \mathcal{X} \to \mathcal{X}$ is a reset map and $u \in \mathcal{U}$ is the controlled input. □

For ease of notation, we will use $f_q(x,u)$ for $f(q,x,u)$. The hybrid quarter car model, obtained by approximating the friction curve μ with a PLF divided in 2 sections, is defined as follows:

$$\dot{x} = f_q(x,u) \tag{14a}$$

$$= -\frac{1}{v}\frac{r}{J}(\Psi_q(x) - u) \tag{14b}$$

$$= -\frac{1}{v}\frac{r^2}{J}F_z\left(m_q x + c_q - \frac{u}{rF_z}\right) \tag{14c}$$

where $x = [\lambda] \in X = [0,1]$ represents the continuous state, $q \in \mathcal{Q} = \{1,2\}$ is the discrete state governed by the switching function (13) and where $u = T_b \in \mathcal{U}$ is the control input (braking torque) which is restricted to the actuation range $\mathcal{U} = [U_{min}; U_{max}]$. It should be noted that the system has no resets ($\rho(q,x) = x$). A graphical representation of this hybrid model can be seen in Fig. 2.

One of the main advantages of the hybrid model (14) is its simplicity: regardless of the discrete state q, the vector field f_q is linear, which facilitates the analysis and the mathematical treatment. For instance, it can be easily shown that the first order system described by (14c) has a time constant given as:

$$\tau_q(v) = \frac{v}{m_q}\left(\frac{J}{r^2 F_z}\right), \quad q \in \mathcal{Q}, \quad m_q \ne 0 \tag{15}$$

This relation shows that the time constant is directly proportional to the vehicle speed v, and affects the slip dynamics: when the vehicle is operating at high speeds the wheel slip λ will respond slowly, while at low speed maneuvers the slip variable will have a much faster response. The discrete state q, and in particulary the slop m_q, also affects the slip dynamics and its stability. For example, the state $q = 2$ is typically characterized by a negative slop, $m_2 < 0$, leading to a negative time constant and instability (pole on the right-side of the plane). On the other hand, the state $q = 1$ has a positive slope, $m_1 > 0$, which leads to a pole in the left-side of the plane ensuring the system stability.

Some of these properties have been already highlighted in previous works (see [2], [5]), using linearized quarter car models around a single working point. However, it's interesting to note that the "multiple linearized" model ($N > 1$), presented in this section and formulated as a hybrid system, extends and improves the precision of the "single-linearized" model ($N = 1$) discussed in [2], [5], which are only valid on a small range around the linearized working point.

IV. HYSTERETIC CONTROLLER

A. Assumptions

During this article, it is assumed the existence of a optimal slip, λ_{SP}, that maximizes the friction coefficient. Normally, the determination of λ_{SP} is difficult to achieve, this leads to the introduction of a tolerance $\Delta\lambda$ when tracking λ_{SP}. This tolerance depends on a number of factors, but experiments carried out by van Zatten [13], shown that the optimal slip should be maintained within the range 8-30%. Additionally, in order to simplify the controller's design, it is assumed that the brake actuator has a negligible response time. Recent actuators, such as the in-wheel electric motors [14], ensure this assumption.

The variable we intent to regulate, slip λ, depends on the wheel ω and vehicle speed v (see (3)). The first variable is easily acquired (with an encoder, for example), but the second one is not easily measured. We'll assume that the vehicle's speed can be estimated [1] or measured experimentally.

B. Controller with Invariance Property

The controller's main objective, maintain the slip λ around a set-point λ_{SP} with a tolerance $\Delta\lambda$, can be formulated as a invariance problem. The invariance specification ensures that the slip is kept within a sub-set of the state space. In the slip control application, the invariant set can be defined as:

$$F = \left\{ x \in [0,1] : \lambda_{min} \leq x \leq \lambda_{max} \right\} \quad (16)$$

where $\lambda_{min} = \lambda_{SP} - \Delta\lambda$ and $\lambda_{max} = \lambda_{SP} + \Delta\lambda$. The invariance of the set F, i.e. $x(t) \in F, \forall t \geq 0$, ensure that the slip will remain in the range $[\lambda_{min}, \lambda_{max}]$, where it is known, in advance, that the friction coefficient is maximized. Figure 3 shows an illustrative example where the invariant set F maximizes the friction coefficient and the lateral friction coefficient is kept within reasonable limits, respecting the controller objectives. Based on the invariance specification, two questions naturally arise: *i)* is there any control law $u(t) \in \mathscr{U}$ that applied to the hybrid system (14) ensures the invariance of set F? *ii)* if so, what is this law? To answer the first question, consider the following proposition:

Proposition 1: Given a Hybrid Systems, like (14), and assuming $x(t_0) \in F \subset X$, there is, at least, one control law that ensures the invariance of set F, i.e. $\forall t > t_0, x(t) \in F$, if the following condition is satisfied:

$$\forall x \in \partial F, q \in \mathscr{Q} \quad \exists u \in \mathscr{U} \quad \text{s.t} \quad \langle x - x_{SP}, f_q(x,u) \rangle \leq 0 \quad (17)$$

where $x_{SP} \in F$ and $\langle .,. \rangle$ is the traditional inner product operator. $\square$

The previous result is presented without proof, but is easily justified since the condition (17) guarantees that, when the state reaches the boundary of the set F, ∂F, the controller has, at least, one entry $u \in \mathscr{U}$, whose vector field will reduce the distance between the state x and the set-point $x_{SP} \in F$.

To design a invariant controller for our slip regulation problem, it is necessary to verify the relationship (17):

$$
\begin{aligned}
L &= \langle x - \lambda_{SP}, f_q(x,u) \rangle \\
&= -\frac{1}{v}\frac{r}{J}(x - \lambda_{SP})(\Psi_q(x) - u) \leq 0 \qquad \forall x \in F, q \in \mathscr{Q}
\end{aligned}
$$

(Note: without loss of validity, the condition $\forall x \in \partial F$ presented in eq. (17) was replaced by a stronger condition $\forall x \in$
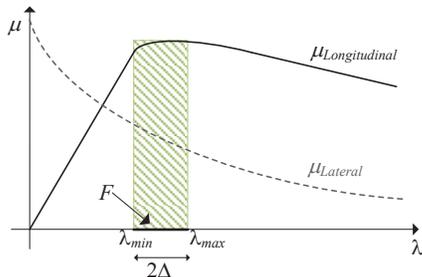

Fig. 3. Definition of the invariant set(F) and representation of the longitudinal and lateral friction coefficient.
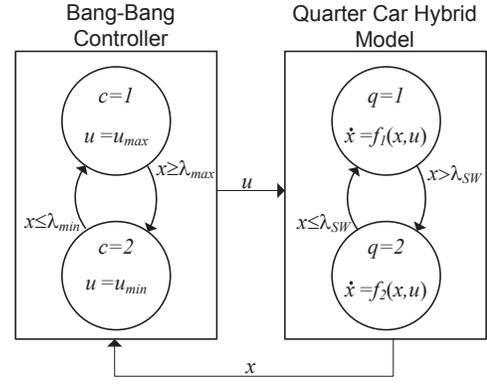

Fig. 4. Hysteretic controller, interconnected with the quarter car hybrid model.

F). The previous equation can be confirmed if $\text{sgn}(x - \lambda_{SP}) = \text{sgn}(\Psi_q - u)$, which is equivalent to:

$$L \leq 0 \Rightarrow \begin{cases} \Psi_q(x) - u \leq 0 & \text{if } x - \lambda_{SP} \leq 0 \\ \Psi_q(x) - u > 0 & \text{if } x - \lambda_{SP} > 0 \end{cases} \quad (18)$$

$$\forall x \in F, q \in \mathscr{Q}$$

If the actuator range $u \in \mathscr{U}_c = [u_{max}; u_{min}] \subset \mathscr{U}$ respect:

$$u_{max} \geq \max_{x \in F, q \in \mathscr{Q}} \Psi_q(x) \quad (19a)$$

$$u_{min} \leq \min_{x \in F, q \in \mathscr{Q}} \Psi_q(x) \quad (19b)$$

then (18) is demonstrated and therefore conditions exists to generate a control law, invariant to set F. Roughly speaking, the actuator range $\mathscr{U}_c$ must cover the upper and lower value of $\Psi_q(x)$ in the domain $x \in F$.

C. Control Law

There are several possible control laws that satisfy the conditions (19). For this work a simple strategy, based on hysteretic control, also known as bang-bang, was used to implement the control law:

$$u^*(t) = \begin{cases} u_{max} & \text{if } x \leq \lambda_{min} \\ u_{min} & \text{if } x \geq \lambda_{max} \\ u(t^-) & \text{otherwise} \end{cases} \quad (20)$$

The controller's principle of operation is as follows: whenever the continuous state reaches or crosses the boundary of the set F, defined by $\partial F = \{\lambda_{min}, \lambda_{max}\}$, a fixed actuator value is selected, $u \in \{u_{max}, u_{min}\}$, constrained by the relations (19a) and (19b) and whose resulting vector field will reduce the distance between x and λ_{SP}. If x belongs to the interior of the set F, then the previous actuator value is maintained. Figure 4 shows an hybrid formulation for the controller described by (20), composed of 2 discrete states, $c \in \mathscr{C} = \{1,2\}$, which define the value u that must be applied to the actuator.
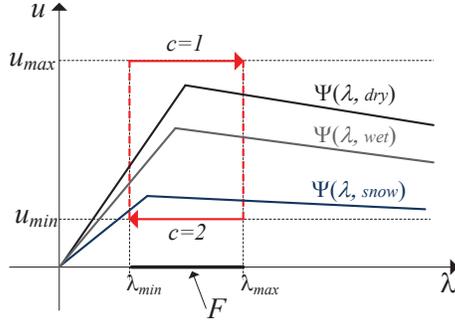
Fig. 5.   Selection of control parameters u_{max} and u_{min} to operate with different grip levels (dry, wet and snow).

D. Disturbances

The friction coefficient between the tire and road, $\mu(\lambda, \theta)$, depends on the adhesion conditions which vary in time and are difficult to estimate with accuracy. Therefore, the friction model is subject to disturbances of the type $\mu(\lambda, \theta \pm d)$, where $d \in \mathcal{D}$ represents the uncertainty in modeling the grip levels, this makes it compulsory to consider the disturbance effects in the derivation of conditions for the existence of a invariant set F, presented in Proposition 1.

Proposition 2: Consider the Hybrid Systems H discussed in the Proposition 1, affected by a disturbance $d \in \mathcal{D}$, which alters the vector field $f_q(x, u, d)$. If

$$\forall x \in \partial F, q \in \mathcal{Q} \qquad \exists u \in \mathcal{U} \qquad \text{s.t}$$
$$\max_{d \in \mathcal{D}} \langle x - x_{SP}, f_q(x, u, d) \rangle \leq 0 \qquad (21)$$

then there is at least one controller which ensures the invariance property of the set F, i.e. $\forall t > t_0, x(t) \in F$, even under the worst disturbance. $\square$

Again, the proposition is given without proof, but the argument for its verification can be easily justified: even if the system is affected by the worst possible adversity, there exists, at least, one control value capable of bringing the system into the interior of set F. Applying the previous proposition to our problem, we obtain the following restriction (equivalent to the relation (18), but including the disturbance effect $d \in \mathcal{D}$):

$$u_{max} \geq \max_{x \in F, q \in \mathcal{Q}} \max_{d \in \mathcal{D}} \Psi_q(x, d) \qquad (22)$$

$$u_{min} \leq \min_{x \in F, q \in \mathcal{Q}} \min_{d \in \mathcal{D}} \Psi_q(x, d) \qquad (23)$$

The previous relations provides tuning rules for the "worst case scenario", where the hysteretic controller must operate on roads with variable grip levels. For example, Fig. 5 shows typical friction curves where the parameters u_{max} and u_{min} were selected taking into account the restrictions (22) and (23). This shows that the parameter u_{max} should be lower limited by the curve with higher friction, dry road conditions for instance, and the parameter u_{min} should be upper limited by the lower adherence conditions, snow for example.

E. Limit Cycle Analysis

The limit cycles are one of the features which arise when certain types of systems are controlled with bang-bang control strategies. It can be easily observed that, if the hysteretic controller respects the inequality (22),(23), then, under closed loop control, the set F is invariant and do not contain any equilibrium point. Therefore, the existence of limit cycle is guaranteed.

The analysis of the limit cycle's period, introduced by the hysteretic controller, is postponed to the next section, where its usefulness for estimating the peak friction will be shown.

V. PEAK FRICTION ESTIMATION

The estimation of the tire-road friction coefficient, μ, is one of the most difficult and challenging tasks in automotive applications. Unlike other physical variables, such as speed, acceleration, yaw-rate, etc., currently there is no economically viable sensor that can be installed on the vehicle to measure the friction coefficient μ. Moreover, μ changes with the varying grip levels present on the road and affects significantly the generation of longitudinal and lateral forces by the tire-road interface. Thus, the estimation of the friction coefficient is of vital importance to improve the performance of active safety systems installed in the vehicle. Besides the ABS, higher control layers, like active torque distribution, yaw rate and side-slip control, can use the friction's estimation to adapt the control strategies according with the current grip levels. The information about road conditions can also be used to alert the driver to potentially dangerous situations [5], [15].

In the following sections we investigate the possibility of obtaining the maximum value of the friction coefficient, μ_{max}, using the limit cycle's period introduced by the hysteretic controller.

A. Hybrid Model Reformulation

Analyzing the typical friction curves generated by (4), usually there exists a zone near the friction peak where the μ derivative, $\partial\mu/\partial\lambda$, is approximately zero, i.e. there is not much variation. Based on this observation, we can increase the number of PLF divisions from two to three
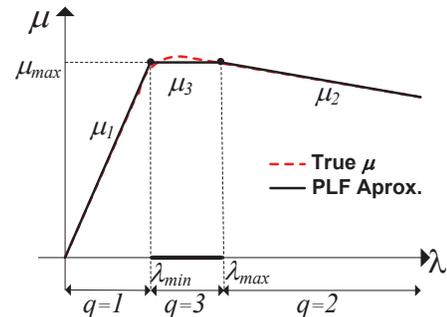

Fig. 6.   Approximation of the friction coefficient μ by a Piecewise Linear Function (PLF) divided in 3 sections.

$(q \in \mathcal{Q} = \{1,2,3\})$, in order to approximate μ, near the zone where $\partial\mu/\partial\lambda \approx 0$, by a constant value. Figure 6 shows the new PLF model, divided in 3 sections. Discrete states $q = 1$ and $q = 2$ have already been described in Section III, and state $q = 3$ has a constant friction value, defined as:

$$\mu_3(\lambda) \quad = \quad m_3\lambda + c_3 = \mu_{max} \tag{24}$$

$$\mu_{max} \quad = \quad \frac{1}{\lambda_{max} - \lambda_{min}} \int_{\lambda_{min}}^{\lambda_{max}} \mu(\lambda)d\lambda \tag{25}$$

It is worth mentioning that the results obtained in the previous section (necessary conditions for a control law with invariance property, disturbance analysis, etc.) remains valid, even increasing the number of discrete states of the hybrid system.

B. Limit Cycle Period

The invariance to the set F, defined by (16), is one of the main properties offered by the hysteretic controller, used to regulate the slip λ. If we match the invariant set F with the invariant condition associated with the discrete state $q = 3$, then for all $x \in F$, the discrete state of the quarter car hybrid model will always be $q = 3$. In other words, we can assume, under closed loop hysteretic control, that the discrete state will be constant and equal to $q = 3$. This approach simplifies the analytical study of the limit cycle's period, since the vector field of λ only depends on the switching performed by the bang-bang controller. In the discrete state $q = 3$, the slip dynamics are given by:

$$\dot{x} \quad = \quad -l(v)(\mu_{max} - u_N) \tag{26}$$

$$l(v) \quad = \quad \frac{1}{v}\frac{r^2}{J}F_z \tag{27}$$

$$u_N \quad = \quad \frac{u}{rF_z} \tag{28}$$

Integrating the equation above, and assuming that the system starts at an initial state λ_0 and reach λ_f in t_f seconds, we get:

$$t_f = \frac{1}{l(v)}\frac{\lambda_0 - \lambda_f}{\mu_{max} - u_N} \tag{29}$$

Replacing λ_0, λ_f and u_N by the boundary conditions, existent in each discrete state of the bang-bang controller, we get the time that the system spent in each state:

$$t_1 = \frac{1}{l(v)}\frac{\lambda_{min} - \lambda_{max}}{\mu_{max} - \frac{u_{max}}{rF_z}} = \frac{2\Delta\lambda}{l(v)}\frac{1}{\left(\frac{u_{max}}{rF_z} - \mu_{max}\right)} \tag{30}$$

$$t_2 = \frac{1}{l(v)}\frac{\lambda_{max} - \lambda_{min}}{\mu_{max} - \frac{u_{min}}{rF_z}} = \frac{2\Delta\lambda}{l(v)}\frac{1}{\left(\mu_{max} - \frac{u_{min}}{rF_z}\right)} \tag{31}$$

where t_1 and t_2 corresponds to the time spent in the state $c = 1$ and $c = 2$, respectively. Summing the previous times, the period of limit cycle is defined as:

$$T \quad = \quad t_1 + t_2 \tag{32}$$

$$= \quad \frac{2\Delta\lambda}{l(v)}\left(\frac{1}{\frac{u_{max}}{rF_z} - \mu_{max}} + \frac{1}{\mu_{max} - \frac{u_{min}}{rF_z}}\right) \tag{33}$$

The equation obtained clearly shows the effects of the parameters v, $\Delta\lambda$ and μ_{max}, in the limit cycle's period. The influence of the vehicle speed in the period T can be analyzed through the term $1/l(v)$ of the previous expression. Since $1/l(v) \propto v$ (see (27)), the period T is also found to be directly proportional to the vehicle's speed, thus a reduction of the cycle's period T is observed when the vehicle's speed decreases. Also the hysteresis band, $2\Delta\lambda$, is found to behave linearly in the period T. Consequently as the hysteresis band decreases the period T decreases as well, which is in line with the "empirical" expectations for a bang-bang control. Lets examine the effects of varying grip levels, by considering the graphs in Fig. 7b. It can be observed that a non-monotonic relation exists between period T and the maximum friction μ_{max}, i.e. for each T there may be two μ_{max} friction values. However, if we analyze the time that the controller spent in each state, t_1 and t_2 (see Fig. 7a), a monotonic relationship can be extracted between t_1 and μ_{max}.

Thus, in order to get an estimation of the maximum friction coefficient, it is necessary to monitor the time that the controller remains in each state, and not the overall period of the limit cycle. Because the controller only has two states, this is equivalent of obtaining the duty cycle of the hysteretic controller.

C. Duty Cycle and Peak Friction

Consider the duty cycle, d, defined as the fraction of time that the controller stays in the state $c = 1$:

$$d \quad = \quad \frac{t_1}{T} = \frac{rF_z\mu_{max} - u_{min}}{u_{max} - u_{min}} \tag{34}$$

Figure 7c presents a graphical representation of the relation between μ_{max} and d, which shows a linear relationship between these variables. Based on this relationship, a simple peak friction estimator can be derived:

$$\hat{\mu}_{max} = \frac{d(u_{max} - u_{min}) + u_{min}}{rF_z} \tag{35}$$

In a way, the resulting equation is quite interesting because it allows for the estimation of the peak friction, knowing only the duty cycle, the braking torque, u_{max} and u_{min}, and the parameters r and F_z. It should be noted that the relationship (35) does not directly depend on the vehicle's speed or the hysteresis band ($\Delta\lambda$); while it does depends on a few physical parameters like the wheel radius and normal force, which can be obtained with reasonable accuracy.

VI. SIMULATIONS

The algorithms developed in this paper were evaluated in a co-simulation between a vehicle dynamics simulation software, the CarSim [16], that has a high order nonlinear model, and the Matlab/Simulink, which allows the implementation of control strategies and the estimation of the peak friction. Unlike the quarter car model used in the controller design, the model used in the vehicle dynamics simulator provides an entire and detailed vehicle model, which allowed for a more realistic testing environment.
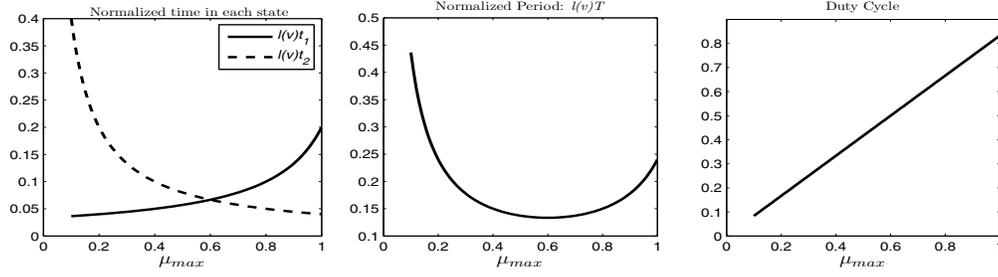
Fig. 7. a) Normalized times t_1, t_2, b) period T and c) duty cycle $d = t_1/T$ under varying peak friction μ_{max} (parameters: $\Delta\lambda = 0.02$, $u_{min} = 0$ and $u_{max} = 1.2rF_z$).

TABLE I

DIMENSIONS AND WEIGHT DISTRIBUTION OF THE TEST VEHICLE

Var.	Description	Value
M	Mass	1230 kg
L	Wheelbase	2.6 m
a	Distance from the CoG to the front axle	1.04 m
b	Distance from the CoG to the rear axle	1.56 m
h	Heigh of the CoG	0.54 m

A. Slip Control

A Hatchback, Class B car, with the main characteristics defined in Table I, was chosen as the test vehicle during these simulations. The original braking system, consisting primarily by hydraulic components, was replaced by in-wheel electric motors, coupled to each of the four wheels, and modeled by a first order system with a delay [14]:

$$G(s) = \frac{T_b}{T_b^*}(s) = e^{-\tau_D s} \frac{1}{\tau_m s + 1} \qquad (36)$$

where T_b^* corresponds to the reference torque generated by the hysteretic controller and T_b is the real braking torque produced by the motor. The time constant τ_m was set at 1ms and the time delay τ_D was given a value of 100us, as in [14]. The tire-road friction model used by the vehicle dynamics simulator is equivalent to the Buckhardt representation (see Section II), and the friction coefficient is maximized in the range $[0.12; 0.18] = F$, regardless of the road adhesion conditions.

To keep the slip in that range, the hysteretic controller was configured with $u_{max} = 1.5rF_z$ and $u_{min} = 0$, in accordance with the restrictions (22) and (23).For simplicity, only the results obtained for the left front wheel of the vehicle are presented (the other wheels have similar behavior). The robustness of the controller against parametric variations is tested applying different grip levels during the braking maneuver (see Fig. 8): the vehicle start braking in a dry surface, but around 1.25s enters in a road covered with snow, featuring less adherence. It can be seen that this disturbance affects the limit cycle period, but the slip is maintained in the optimal range, ensuring the invariance property.
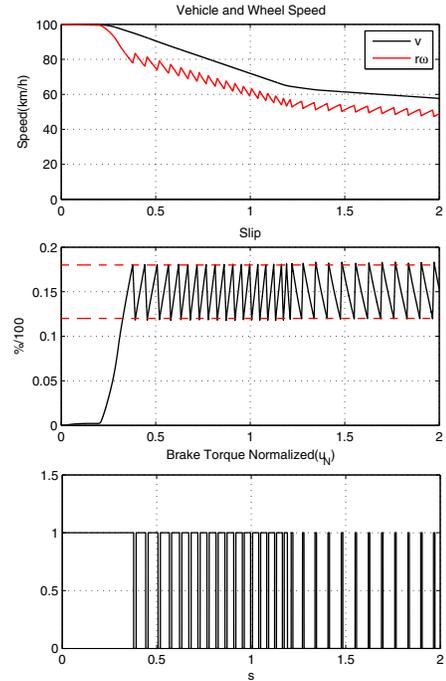

Fig. 8. Braking in a variable grip surface with ABS active (from 0 to 1.25s the road is dry and, afterwards, is covered with snow).

B. Peak Friction Estimation

To evaluate the peak friction's estimation, a more demanding test with 3 types of road adhesion conditions (dry, wet and snow) was performed. The braking maneuver started in a dry road, and then changed to wet and snow. Figure 9 illustrates the evolution of the controller's duty cycle and peak tire-road friction estimation μ_{max} during this experiment. It can be observed that the duty cycle decreases with the degradation of the adhesion conditions, something that was theoretically expected due to the relationship (34) (see Fig. 7). The peak friction estimation, μ_{max}, presents an excellent performance and was able to track the transitions from dry ($\mu_{max} \approx 1$) to wet ($\mu_{max} \approx 0.65$) and to snow ($\mu_{max} \approx 0.2$). It should be noted that while the limit cycle does not stabilize, which only occurs around 0.35s, the estimate of μ_{max} produced erroneous estimations that should
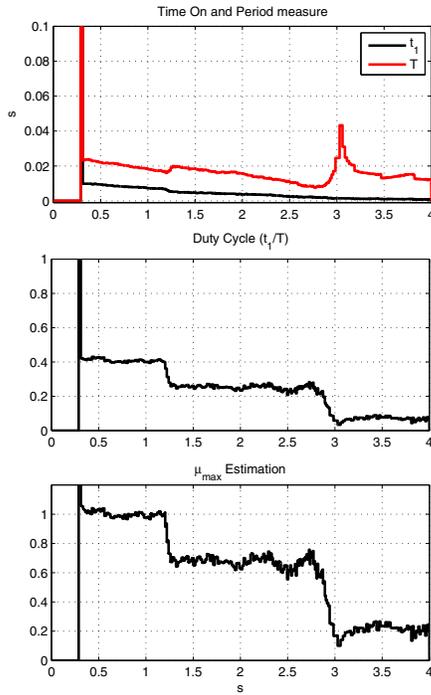
Fig. 9. Duty cycle of the hysteretic control and friction estimation (μ_{max}) during braking in the dry-wet-snow test.

be discarded.

VII. CONCLUSIONS

This paper addressed the tire slip control problem and the peak friction estimation, with a full hybrid framework. The nonlinearity present in the tire-road friction coefficient was approximated by a Piecewise Linear Function (PLF), motivating the introduction of a hybrid model to represent the vehicle dynamics. Based on this hybrid framework, the slip regulation was formulated as an invariant problem which can be resolved by a hysteretic controller. The main merit of hysteretic controller is its robustness to the model's parametric variations, such as the grip levels present on the road. By analyzing the properties of the close loop hybrid system, in particular the limit cycle's period, we noticed that it is possible to extract a linear relationship between the controller's duty cycle and the peak friction coefficient. One of the main features of this estimator is that it does not directly depend on the vehicle longitudinal velocity and only requires simple parameters like the wheel radius and normal force. Thus, through the monitoring of the controller's duty cycle, it was possible to infer the grip levels present on the road. Simulation results, obtained with a vehicle dynamics simulation software, demonstrated a good performance of the proposed methods.

Future efforts include the possibility of incorporate adaptive mechanisms to modify the hysteretic controller parameters, u_{max} and u_{min}, taking into account the conditions of adhesion obtained with the estimator.

REFERENCES

[1] U. Kiencke and L. Nielsen, *Automotive Control Systems For Engine, Driveline, and Vehicle*. Springer, 2005.
[2] S. M. Savaresi, M. Tanelli, and C. Cantoni, "Mixed slip-deceleration control in automotive braking systems," *Journal of Dynamic Systems, Measurement, and Control*, vol. 129, no. 1, pp. 20–31, 2007.
[3] W. Pasillas-Lepine, "Hybrid modeling and limit cycle analysis for a class of five-phase anti-lock brake algorithms," *Vehicle System Dynamics: International Journal of Vehicle Mechanics and Mobility*, vol. 44, no. 2, pp. 173–188, 2006.
[4] T. A. Johansen, I. Petersen, J. Kalkkuhl, and J. Ludemann, "Gain-scheduled wheel slip control in automotive brake systems," *Control Systems Technology, IEEE Transactions on*, vol. 11, no. 6, pp. 799–811, 2003.
[5] Y. Hori, "Future vehicle driven by electricity and control - research on four-wheel-motored "uot electric march ii," *IEEE Transactions on Industrial Electronics*, vol. 51, no. 5, pp. 954–962, 2004.
[6] S. Drakunov, U. Ozguner, P. Dix, and B. Ashrafi, "Abs control using optimum search via sliding modes," *IEEE Transactions on Control Systems Technology*, vol. 3, no. 1, pp. 79–85, 1995.
[7] L. Li and F.-Y. Wang, *Advanced motion control and sensing for intelligent vehicles*. Springer Verlag, 2007.
[8] M. Schinkel and K. Hunt, "Anti-lock braking control using a sliding mode like approach," in *American Control Conference. Proceedings of the*, vol. 3, 2002, pp. 2386–2391.
[9] F. Borrelli, A. Bemporad, M. Fodor, and D. Hrovat, "An mpc/hybrid system approach to traction control," *Control Systems Technology, IEEE Transactions on*, vol. 14, no. 3, pp. 541–552, 2006.
[10] M. Tanelli, G. Osorio, M. di Bernardo, S. M. Savaresi, and A. Astolfi, "Existence, stability and robustness analysis of limit cycles in hybrid anti-lock braking systems," *International Journal of Control*, vol. 82, no. 4, pp. 659–678, 2009.
[11] H. B. Pacejka, *Tyre and vehicle dynamics*. Butterworth-Heinemann, 2002.
[12] C. Canudas-de Wit, P. Tsiotras, E. Velenis, M. Basset, and G. Gissinger, "Dynamic friction models for road/tire longitudinal interaction," *Vehicle System Dynamics*, vol. 39, no. 3, pp. 189–226, 2003.
[13] A. van Zanten, R. Erhardt, and A. Lutz, "Measurement and simulation of transients in longitudinal and lateral tire forces," *SAE Trans.*, vol. 99, no. 6, pp. 300–318, 1990.
[14] S. I. Sakai, H. Sado, and Y. Hori, "Anti-skid control with motor in electric vehicle," in *Advanced Motion Control, 2000. Proceedings. 6th International Workshop on*, 2000, pp. 317–322.
[15] S. Muller, M. Uchanski, and K. Hedrick, "Estimation of the maximum tire-road friction coefficient," *Journal of Dynamic Systems Measurement and Control-Transactions of the Asme*, vol. 125, no. 4, pp. 607–617, 2003.
[16] "Carsim user manual," *Mechanical Simulation Corporation*, 2008, http://www.carsim.com.